ICSBE2016-58

DAMAGE DETECTION OF CORRODED STEEL SPECIMENS BY USING MACHINE LEARNING APPROACH

C. N. N. Karina[1] and P. Chun[1*]

[1]*Ehime University, Matsuyama, Japan*
**E-mail: chun@cee.ehime-u.ac.jp, TP: +81899279822*

Abstract: Safety service improvement and the development of an efficient maintenance strategy for corroded steel structures are undeniably essential. Therefore, understanding the influence of damage caused by corrosion on the remaining load-carrying capacities such as tensile strength is required. In this study, artificial neural networks (ANNs) approach is proposed in order to produce a simple, accurate, and inexpensive method developed by using tensile test results, material properties and finite element method (FEM) results to train the ANNs model. Initially in reproducing corroded model process, FEM was used to obtain tensile strength of artificial corroded plates of which surface is developed by a spatial autocorrelation model. By using the corroded surface data and material properties as input data, with tensile strength as the output data, the ANNs model could be trained. The accuracy of the ANNs result was then verified by using leave-one-out cross-validation (LOOCV). Hence, the proposed ANNs model now enables us to have a simple, rapid, and inexpensive method to predict residual tensile strength more accurately due to corrosion in steel structures.

Keywords: Artificial neural networks; corrosion; finite element analysis; tensile test

1. Introduction

Many steel bridge infrastructures are subjected to corrosion due to exposure to aggressive environmental conditions and inadequate maintenance (Kaita et al., 2012). Corrosion has a harmful consequence from the safety point of view and can lead to thickness penetration, fatigue cracks, brittle fracture and unstable failure (Khedmati et al., 2011). Evaluation of existing steel structures due to deterioration caused by corrosion, natural aging, increasing load spectra, increasing seismic demand, and other problems becomes vital (Ohga, et.al 2011). Therefore, understanding the influence of damage on the remaining load-carrying capacities is required.

2. Verification of the Validity of Finite Element Method (FEM) by a Tensile Experiment on Corroded Steel Plates

2.1 Corroded Plate Thickness Measurement

The test specimens were cut out from steel girders of the Ananai River Bridge in Kochi Prefecture and Funakoshi Bridge in Ehime Prefecture in Japan. There were 30 corroded steel specimens in total: 18 from Ananai Bridge, and 12 from Funakoshi Bridge. The specimens named as ANT-1~ANT-18, FUT-1~FUT-12, belonged to Ananai Bridge and Funakoshi Bridge respectively. The first two letters of the coding name rule are taken from the first two letters of the bridge name and the last letter of T is taken from the first letter of 'Tensile test'.

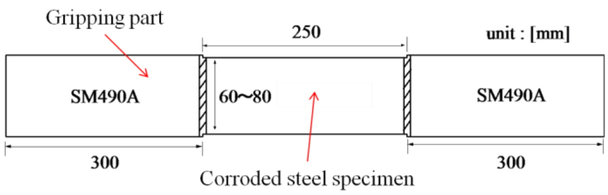

Fig 01: Corroded test specimens

Before conducting the thickness measurement, all the rust over both surfaces was removed carefully by using electric wire brushes and punches. Then, new SM490A plates were jointed to both end surface sides of the specimen by butt full penetration welding for the gripping parts to be placed on the loading machine, as shown in Figure 1. In addition, six corrosion-free-specimens (JIS5 type) were made, three each from the Ananai Bridge and Funakoshi Bridge, and tensile tests were carried out to clarify the material properties of the test specimens. The

Table 1: Material Properties

Specimens	Modulus Elasticity (GPa)	Poisson's ratio	Yield Stress (MPa)	Tensile strength (MPa)	Fracture Elongation (%)
Ananai Bridge	197.4	0.272	281.6	431.3	40.2
Funakoshi Bridge	208	0.280	280.0	437.6	40.6

material properties obtained from these tests are shown in Table 1. Furthermore, since accuracy and convenience are highly demanded in the measurement of corroded surface irregularities, a portable three-dimensional (3D) scanning system was used in this surface measurement, as shown in Figure 2(a). The 3D measuring device allows us to measure 3D coordinate values at any arbitrary point on a corroded surface directly and continuously (Kaita et al, 2005). The device can measure the coordinates of a point on a steel surface by using a non-contact scanning probe (laser line probe). The situation of when measuring the corroded thickness is shown in Figure 2(b).

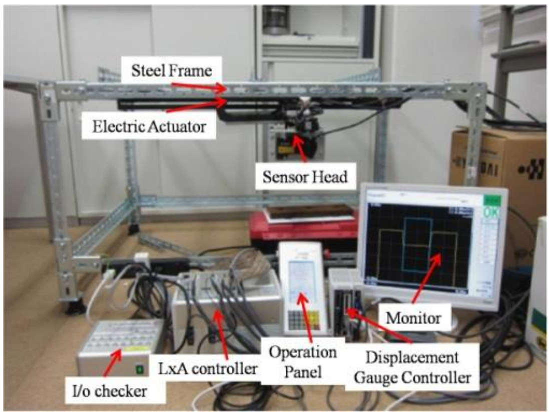

(a) 3D laser measuring device

(b) Thickness measurement by 3D measuring device

Fig 02: Measuring device and thickness measurement by 3D measuring device

2.2 Tensile Test of Corroded Steel Specimens

Tensile tests were carried out under loading control at a constant velocity by using a hydraulic loading test machine (maximum load: 2940 kN) for all 30 specimens, with different levels of corrosion. The loading velocity was set to 150 N/s to avoid dynamic failure. One of the prepared specimens with already attached strain gauges on it can be seen in Figure 3.

Fig 03: Specimen prepared for tensile test

2.3 Verification of the Validity of FEM

In this study, FEM was examined by comparing the results to the tensile test results, as shown in Figure 4. Finite element analysis (FEA) has been used to reproduce many corroded surface shapes by using a spatial autocorrelation model in order to train the ANNs model. Figure 4(a) indicates that tensile strength values between FEM and experiment were almost equivalent. As for comparison results for specimen ANT-8 can be seen in Figure 4(b) which shows a very good agreement in load and displacement curves between FEM results and the experimental results. These comparison results prove that FEM model is very well validated, and the FEM model can be used for developing ANNs model

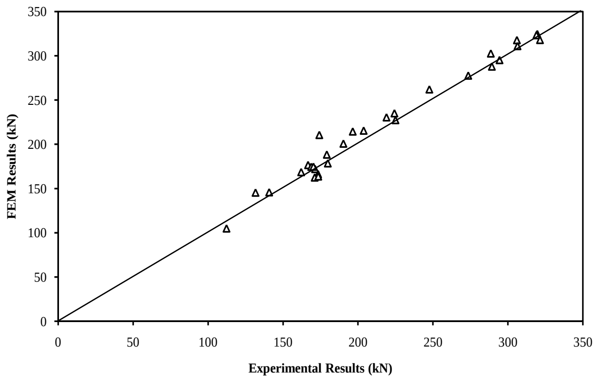

(a) Comparison of tensile strength results

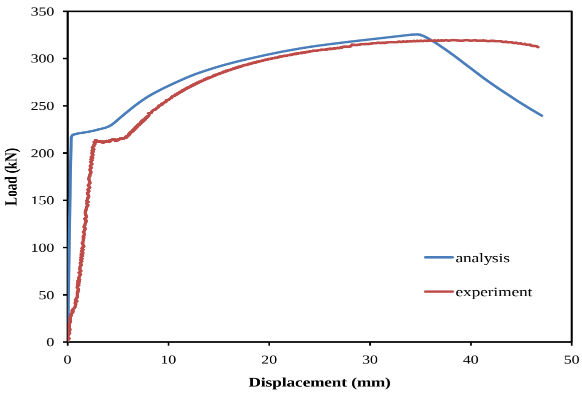

(b) Load-displacement curves for ANT-8

Figure 4: Comparison results between FEM results and experimental results

3. Structure of Training Data Set

A spatial autocorrelation model was made by taking into account the correlation between the corrosion depth of each node on the corrosion surface. By Equation (1), the corrosion depth distribution was derived, where V_i' is the corrosion depth at the *i-th* measurement point, V_i is the independent corrosion depth at the *i-th* measurement point, β is the distance attenuation coefficient, and d_{ij} is the distance between point i and point j. By referring to Okumura et al., β values are between 0.28 and 0.4 and in this study β values were set randomly between those values. As for the parameter range, it is shown in Table 2.

The V_i values are independent and randomly generated from Poisson distribution (Fujii et al., 2001). Therefore, in real situation, V_i values and V_j values are close to each other in real situation, the values maybe similar. In order to include this condition, $e^{-\beta d_{ij}}$ is applied to the Equation (1). Hence, it is expected that when $e^{-\beta d_{ij}}$ values get bigger, d_{ij} values get smaller, which means, ne value at point i (V_i') is affected by V_j considerably if point i and point j are close to each other. In this way, the depth distribution values of V_1' to V_n' can be more natural since two points are close to each other which have similar values

$$\begin{pmatrix} V_1' \\ V_2' \\ \vdots \\ V_n' \end{pmatrix} = \begin{pmatrix} 1 & e^{-\beta d_{21}} & \cdots & e^{-\beta d_{n1}} \\ e^{-\beta d_{12}} & 1 & \cdots & e^{-\beta d_{n2}} \\ \vdots & \vdots & \ddots & \vdots \\ e^{-\beta d_{1n}} & e^{-\beta d_{2n}} & \cdots & e^{-\beta d_{nn}} \end{pmatrix} \begin{pmatrix} V_1 \\ V_2 \\ \vdots \\ V_n \end{pmatrix} \tag{1}$$

In this study, a pitting corrosion case was also generated by creating oval-shaped corrosion and general corrosion case on the plate surface randomly using autocorrelation model as shown in Figure 5. A 2-mm regular mesh pattern was adopted for all the analytical models. One edge of the member's translation in the *x*-, *y*-, and *z*-directions was fixed and only the *y*-, and *z*-direction translations of the other edge (loading edge) were fixed, to simulate the actual experimental conditions. Uniform incremental displacement was then applied to the loading edge.

Table 2: Parameters taken from measurement and experimental results

Parameter	Range
Initial thickness [mm]	10.0~40.0
Width [mm]	20.0~150.0
Length [mm]	202.0~1500.0
Average thickness [mm]	4.6~36.6
Minimum average thickness [mm]	1.6~33.5
Minimum thickness [mm]	0.003~27.9
Standard deviation [mm]	0.172~5.307
Young modulus [GPa]	180.0~219.8
Yield strength [MPa]	200.0~290.0
Ultimate strength [MPa]	390.0~520.0

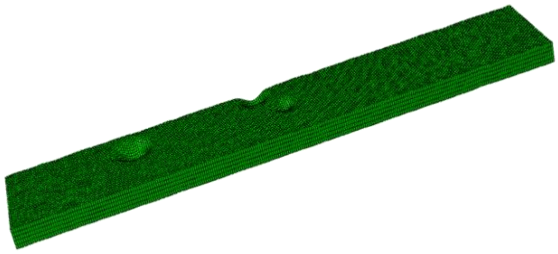

(a) Pitting corrosion case

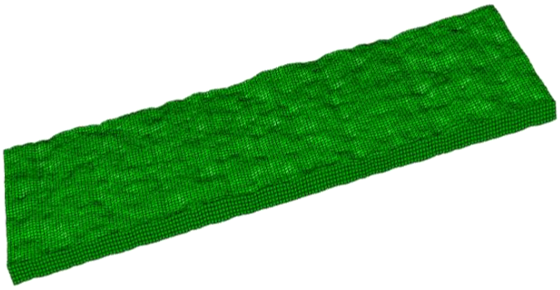

(b) Average corrosion case

Figure 5: Artificial corroded models reproduced by spatial autocorrelation model

4. Framework of Artificial Neural Network

4.1 Overview of Artificial Neural Network

The tensile strength prediction method has been developed by using a multilayer perceptron feed-forward artificial neural network as depicted in Figure 6. ANNs consists of multiple layers including an input layer, hidden layer(s), and an output layer. These layers have nodes interconnected with the nodes of adjoining layers by synapses. Figure S in the Figure 6 is the activation function which is chosen as the sigmoidal function as formulated in Equation (2

$$S(a) = \frac{2}{1+\exp(-2a)} - 1 \quad (2)$$

The synaptic weight is updated in order to increase the accuracy of neural network by minimizing the sum-squared error norm $E(\mathbf{w})$ as shown in Equation (3).

$$E(\mathbf{w}) = \frac{1}{2}\sum_{n=1}^{N}\left\|\mathbf{y}(\mathbf{x}_n,\mathbf{w}) - \mathbf{t}_n\right\|^2 \quad (3)$$

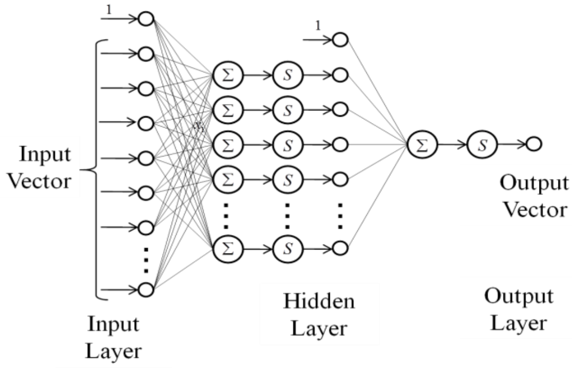

Fig 06: Typical feed-forward artificial neural network

$\mathbf{w}$ is the synaptic weight vector, $\mathbf{x}_n$ is a set of input vectors, $\mathbf{y}(\mathbf{x}_n, \mathbf{w})$ is the vector of output variables, $\mathbf{t}_n$ is a corresponding set of target vectors, N is the number of data set (input-output). Though the Back-propagation algorithm is a well-known algorithm to minimize $E(\mathbf{w})$ in Equation (3), the formula still lacks computation speed. Therefore, in this study, the Levenberg-Marquardt optimization algorithm has been used because it performed better than other algorithms in terms of convergence rate (El-Bakyr, 2003). In the Levenberg-Marquardt algorithm, the weight vector can be adjusted iteratively as given in Equation (4).

$$\mathbf{w}^{(r+1)} = \mathbf{w}^{(r)} - \left[\mathbf{J}^T\mathbf{J} + \mu\mathbf{I}\right]^{-1}\mathbf{J}^T\mathbf{e} \quad (4)$$

$\mathbf{e}$ is the error vector, $\mathbf{J}$ is the Jacobian matrix which contains the first derivatives of the error $\mathbf{e}$ in the network by means at weights $\mathbf{w}$ and bias, $\mathbf{I}$ is the identity matrix, r is the number of iterations, μ is the Marquardt parameter, and in this study, 0.001 was used as an initial value.

4.2 Accuracy Verification

LOOCV is a validation method that will train all the data except for one datum and the prediction will be made for that one datum (Bishop C.M , 2007). This process was repeated until the rest of the overall data set had been trained. As discussed previously, in this study, 1000 data sets (input-output) were prepared. ANNs was trained primarily by using only 999 data due to the one datum was taken out from the data set to be analyzed. This process was repeated 1000 times until all data sets had been evaluated in order to verify the accuracy of ANNs results. Moreover, the mean absolute error percentage was also derived by using the following Equation (5) to evaluate the performance quantitatively. In the equation below, N is the number of data set (input-output), y_t is the target data, and y_p is the predicted result.

$$\text{Mean absolute error percentage} = \frac{1}{N}\sum_{i=1}^{N}\left|\frac{y_t - y_p}{y_t}\right| \quad (5)$$

In this study, it is necessary to investigate the relationship of all ten parameters mentioned in the previous section to analyse the result by considering five different cases as shown in the following list, and the validation results can be seen in Figs. 7 to 9 for cases 1 to 3 respectively. The error percentages derived from Equation (5) are summarized in Table 3.

1. All parameters were included

2. Average thickness, plate width, plate length, initial thickness, young modulus, ultimate strength, yield strength were included

3. Parameters in case 2 and minimum average thickness were included

Table 3 and the comparison of predicted results between FEM and ANNs for each case show that the error percentage increased significantly when the information on minimum average thickness was taken away from input data, as seen in case 2. Since case 1 and case 3 have minimum average thickness data, the error percentages are small. This results show that the information on minimum average thickness is crucial in order to achieve an accurate result. In case 1 and case 3, theANNs result gives a very accurate result by being able to produce a mean absolute error percentage below 5%. These results prove that the ANNs accuracy of case 1 and case 3 is validated. Therefore, ANNs approach now enables us to replace

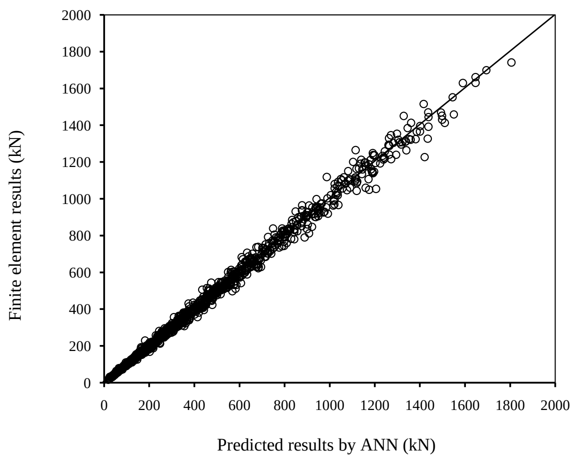

Fig 07: Comparison predicted results of FEM and ANNs for case 1

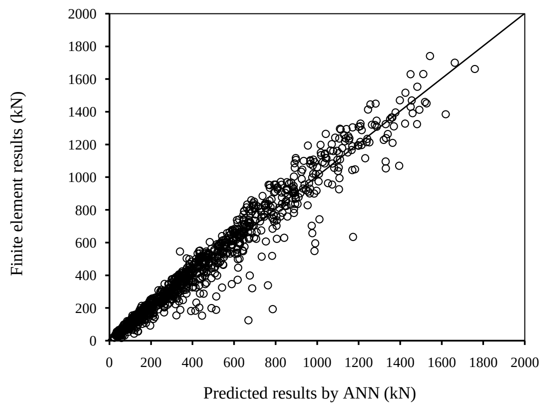

Fig 08: Comparison predicted results of FEM and ANNs for case 2

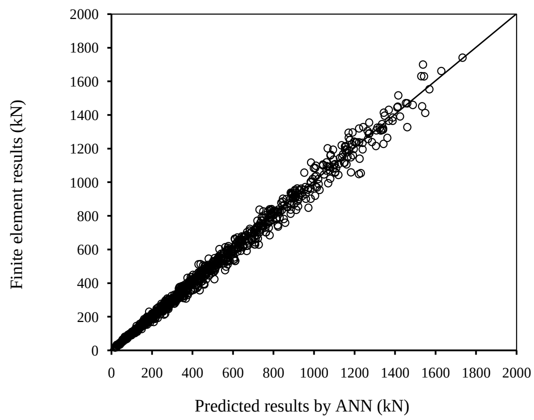

Fig 09: Comparison predicted results of FEM and ANNs for case 3

Table 3: The percentage of mean absolute error percentage for each case

	Mean absolute error percentage %
Case 1	3.7%
Case 2	15.4%
Case 3	4.6%

previous approaches such as experimental studies and costly analytical study. Time-consuming and expensive cost problems are solved by the ANNs approach.

5. Conclusions

In this study, corroded surface data, material properties and FEM results were used to train the ANNs model and the accuracy of the model was verified by leave-one-out cross-validation. Initially, in order to verify the FEM, FEM results were compared to experimental results. It was confirmed that the FEM results were accurate. Thereby, the finite element method could then be used to import corroded surface data developed by the spatial autocorrelation model and the artificial corroded models were then analysed by FEA to obtain tensile strength information. By using the information from corroded surface data, material properties and tensile strength, the ANNs model could then be trained. The ANNs results were then compared to FEM results by considering five different cases applied in this study. Cases 2 has a large mean absolute error percentage due to lack of minimum average thickness information, while cases 1 and 3 have a very small mean absolute error percentage with minimum average thickness information included in the ANNs model. This shows that minimum average thickness information is crucial in determining the accuracy of ANNs results. It is suggested to always include minimum average thickness information in this proposed approach. With this information, cases 1 and 3 could produce a mean absolute error percentage below 5%. Therefore, in this study, case 1 is selected to confirm the accuracy of the ANNs approach. Thus, the ANNs approach can be considered as a simple, rapid, and inexpensive method to predict residual tensile strength more accurately.

Acknowledgement

The authors are feeling very grateful for Ehime University that facilitated us to make this research could be conducted well followed by every individual in Structural engineering laboratory involved in research activities. This research would never be done successfully without their contribution.

References

[1]. Bishop, C.M., "Pattern Recognition and Machine Learning", Springer, Japan, 2007.

[2]. El-Bakyr M.Y., "Feed forward neural networks modeling for K-P interactions, Chaos, Solutions & Fractals", Vol. 18, No. 3, pp. 995-1000, 2003.

[3]. Kaita, T., Tagaya, K., Fujii, K.,Miyashita,M., and Uenoya, M., "A simple estimation method of bending strength for corroded plate girder." Collaboration and Harmonization in Creative Systems, 1, Taylor & Francis, London, pp. 89-97, 2005.

[4]. Kaita, T., Appuhamy, J.M.R.S., Ohga, M., and Fujii, K., "An enhanced method of predicting effective thickness of corroded steel plates." Steel and Composite Structures, Vol. 12, No.5, pp. 379-393, 2012.

[5]. Khedmati, M.R., Nouri, Z.H.M.E., and Roshanali, M.M., "An effective proposal for strength evaluation of steel plates randomly corroded on both sides under uniaxial compression." Steel and Composite Structure, Vol.11, No.3, pp. 183-205, 2011.

[6]. Ohga, M., Appuhammy, J.M.R.S., Kaita, T., Chun, P., and Dissanayake, P.B.R., "Degradation of Tensile Strength with the Severity of Corrosion Condition." World Congress on Advances in Structural Engineering and Mechanics (ASEM11plus), Seoul, Korea, pp. 5280-5297, 2011.

[7]. Okumura, M., Fujii, K., and Tukai, M., "Statistical model of steel corrosion considering spatial auto-correlation" Journal of JSCE, 672/VI-50, pp. 109-116, 2001 (in Japanese).